Mathematics of super-resolution biomedical imaging

Habib Ammari

Department of Mathematics, ETH Zürich

Mathematics for biomedical imaging

- Biomedical imaging:
  - Image electrical, optical, and mechanical tissue properties using electromagnetic and elastic waves at single or multiple frequencies.
  - Enhance the resolution, the stability, and the specificity.
- Direct and inverse problems for wave propagation in complex media.
- Build mathematical frameworks and develop effective numerical algorithms for biomedical imaging applications.

Mathematics for biomedical imaging

- Key concepts:
  - Resolution: smallest detail that can be resolved.
  - Robustness: stability of the image formation with respect to model uncertainty and electronic noise.
  - Specificity: physical nature (benign or malignant for tumors).

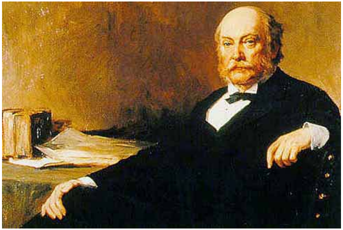

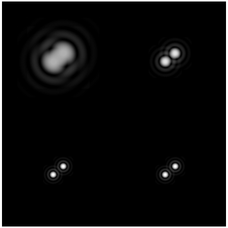

Mathematics for biomedical imaging

- Waves play a key role in biomedical imaging techniques.
- Visualize contrast information on the electrical, optical, mechanical properties of tissues.
- Tissue contrasts:
  - Highly sensitive to physiological and pathological tissue status.
  - Depend on the cell organization and composition.
  - Overall parameters, averaged in space over many cells.
- Recognize the microscopic cell organization and composition from measurements at the macroscopic level.

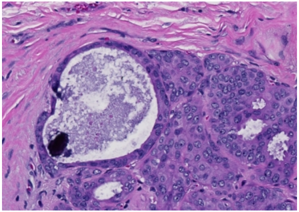

Mathematics for biomedical imaging

- Diagnosis and staging of cancer disease.
- Help surgeons to make sure they removed everything unwanted around the margin of the cancer tumor.
- Perform biopsy in the operating room.

Imaging electrical properties of tissues

- Magnetic permeability $\mu =$ free space $= 1$.
- Electrical conductivity σ: tissue's ability to transport charges;
- Electrical permittivity (dielectric constant) ε': tissue's ability to trap or to rotate molecular dipoles; determined by the polarization under an external electric field; free space electrical permittivity $= 1$.
    - σ and ε': frequency-dependent or dispersive; ω: frequency of the alternating current.
    - Capacitive effect generated by the cell membrane structure.
    - $\sigma(\omega) = \sigma_0 + \omega\varepsilon''(\omega)$; ε'': loss factor; σ_0: conductivity at very low frequencies.
    - $\varepsilon(\omega) = \varepsilon'(\omega) - i\omega\varepsilon''$: complex permittivity.
- Electrical admittivity $\kappa = \sigma + i\omega\varepsilon'$; macroscopic parameter; represents the electrical properties of the tissue averaged in space over many cells; can be anisotropic.

Imaging electrical properties of tissues

- Causality $\Rightarrow$ Kramers-Krönig relations (Hilbert transform):

$$\varepsilon'(\omega) - \varepsilon_\infty = -\frac{2}{\pi}\text{p.v.} \int_0^{+\infty} \frac{s\varepsilon''(s)}{s^2 - \omega^2} ds,$$

$$\varepsilon''(\omega) = \frac{2\omega}{\pi}\text{p.v.} \int_0^{+\infty} \frac{\varepsilon'(s) - \varepsilon_\infty}{s^2 - \omega^2} ds,$$

- ε_∞: dielectric constant at very high frequencies.

Imaging electrical properties of tissues

- Dispersion: significant change in the dielectric properties over a frequency range.
- Relaxation mechanisms (depend on the tissue):
    - α-dispersion: low frequencies (80 Hz for muscle)
    - β-dispersion: radio frequencies (50 KHz)
    - γ-dispersion: microwave frequencies (25 GHz); σ increases with ω (dipolar reorientation of tissue water); ε' decreases.

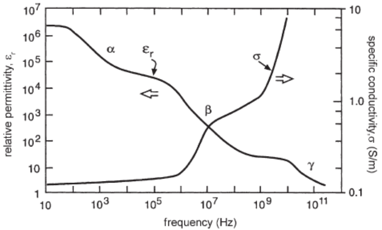

Imaging electrical properties of tissues

- Empirical approaches:
  - Debye model:
  $$\varepsilon(\omega) = \varepsilon_\infty + \frac{\varepsilon_0 - \varepsilon_\infty}{1 + i\omega\tau}$$
  - Cole-Cole model:
  $$\varepsilon(\omega) = \varepsilon_\infty + \frac{\varepsilon_0 - \varepsilon_\infty}{1 + (i\omega\tau)^\alpha}$$
  - ε_0: dielectric constant at very low frequencies; τ: relaxation time; τ and $0 < \alpha < 1$: depend on the nature of the biological material.

Imaging electrical properties of tissues

- Maxwell's equations:

$$\begin{cases} \nabla \times E = -\dfrac{\partial H}{\partial t}, \quad \nabla \times H = J + \dfrac{\partial D}{\partial t}, \\ \nabla \cdot H = 0, \quad \nabla \cdot D = \rho. \end{cases}$$

- Equation of conservation of charge:

$$\nabla \cdot J + \frac{\partial \rho}{\partial t} = 0.$$

- Ohm's law:

$$J = \sigma_0 E \quad \text{in } \Omega \times \mathbb{R}_+. \tag{1}$$

- Total current density $J_{\mathrm{tot}} = J + \partial D/\partial t = \sigma_0 E + \partial D/\partial t$.
- Causal constitutive relationship:

$$D(x,t) = \int_{-\infty}^{t} \varepsilon(x, t-s) E(x,s) ds, \quad (x,t) \in \Omega \times \mathbb{R}^+.$$

Imaging electrical properties of tissues

- Time-harmonic solutions:

$$E(x,t) = \frac{1}{\sqrt{2\pi}} \int_{-\infty}^{+\infty} E(x,\omega) e^{i\omega t}\, d\omega, \quad H(x,t) = \frac{1}{\sqrt{2\pi}} \int_{-\infty}^{+\infty} H(x,\omega) e^{i\omega t}\, d\omega.$$

- Constitutive relation:

$$D(x,\omega) = \varepsilon(x,\omega) E(x,\omega).$$

- Kramers-Kronig relations: frequency-domain expression of causality.
- Maxwell equations:

$$\nabla \times \nabla \times E - \omega^2 \big(\varepsilon' + i\frac{\sigma}{\omega}\big) E = 0.$$

- $\omega \to 0$, $E = \nabla u$: u solution to the conductivity equation

$$\nabla \cdot \big(\sigma + i\omega\varepsilon'\big) \nabla u = 0.$$

- Microwave frequencies (slow variations of ε), E_j solution to the Helmholtz equation:

$$\Delta E_j + \omega^2 \big(\varepsilon' + i\frac{\sigma}{\omega}\big) E_j = 0.$$

Imaging optical properties of tissues

- Optical propagation in biological tissues: three scales.
  - Maxwell's equations in random media: microscopic scale.
  - Radiative transport equation (RTE): mesoscale.
  - Diffusion approximation to the RTE: macroscale.
- Absorption coefficient μ_a; Scattering coefficient μ_s; depend on the wavelength.
- Fluence rate:

$$\frac{1}{c}\frac{\partial \Psi}{\partial t} - \nabla \cdot \left[\frac{1}{3(\mu_s + \mu_a)} \nabla \Psi \right] + \mu_a \Psi = 0.$$

- Fluence: integral over time of Ψ.

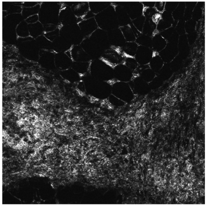

Imaging elastic properties of tissues

- (λ, μ): Lamé coefficients; ρ: density.
- Lamé system:

$$\begin{cases} \rho \dfrac{\partial u}{\partial t^2} - \nabla \lambda \nabla \cdot u - \nabla \cdot \mu \nabla^s u = F & \text{in } \Omega \times \mathbb{R}_+, \\ \dfrac{\partial u}{\partial n} = 0 & \text{on } \partial\Omega \times \mathbb{R}_+, \\ u(x,0) = \dfrac{\partial u}{\partial t}(x,0) = 0 & \text{in } \Omega. \end{cases}$$

- $\nabla^s = (\nabla + \nabla^T)/2$; T: transpose.
- Co-normal derivative: $\frac{\partial u}{\partial n} = \lambda(\nabla \cdot u)\nu + 2\mu \nabla^s u \, \nu$.
- Strain tensor: $\nabla^s u$.
- Elasticity tensor: $C_{ijkl} = \lambda \delta_{ij}\delta_{kl} + \mu(\delta_{ik}\delta_{jl} + \delta_{il}\delta_{jk})$.
- Stress tensor: $\sigma(u) = \mathbb{C}\nabla^s u$.

Imaging elastic properties of tissues

- $\mu = 0$: dominant wave type is a compressional wave.
- Pressure $p = \lambda \nabla \cdot u \quad$ in $\Omega \times \mathbb{R}_+$.
- Acoustic wave equation:

$$\begin{cases} \dfrac{1}{\lambda}\dfrac{\partial^2 p}{\partial t^2} - \nabla \cdot \dfrac{1}{\rho}\nabla p = \nabla \cdot F \quad \text{in } \Omega \times \mathbb{R}_+, \\ p = 0 \quad \text{on } \partial\Omega \times \mathbb{R}_+, \\ p(x,0) = \dfrac{\partial p}{\partial t}(x,0) = 0 \quad \text{in } \Omega. \end{cases}$$

- Time-harmonic regime:

$$\begin{cases} \nabla \cdot \dfrac{1}{\rho}\nabla p + \dfrac{\omega^2}{\lambda} p = -\nabla \cdot F \quad \text{in } \Omega, \\ p = 0 \quad \text{on } \partial\Omega. \end{cases}$$

- Density ρ: ultrasound imaging.

Imaging elastic properties of tissues

- Time harmonic regime:

$$\begin{cases} \nabla \cdot \mu \nabla^s u + \nabla \lambda \nabla \cdot u + \omega^2 \rho u = F & \text{in } \Omega, \\ \dfrac{\partial u}{\partial n} = 0 & \text{on } \partial\Omega. \end{cases}$$

- Shear modulus μ: stiffness depends on the tissue composition; related to abnormal phatological processes.
- Compressional modulus λ: 4 order of magnitude larger than μ.
- Modified Stokes system as $\lambda \to +\infty$:

$$\begin{cases} \nabla \cdot \mu \nabla^s u + \nabla p + \omega^2 \rho u = F & \text{in } \Omega, \\ \nabla \cdot u = 0 & \text{in } \Omega, \\ p\nu + \mu \dfrac{\partial u}{\partial \nu} = 0 & \text{on } \partial\Omega. \end{cases}$$

- Remove the compression modulus from consideration.
- Viscosity tissue properties: real and imaginary parts of μ connected by Kramers-Kronig relations.

Mathematics for biomedical imaging

- Anomaly imaging: take advantage of the smallness of the imaged anomalies.
- Hybrid imaging: one single imaging system based on the combined use of conductivity imaging and acoustic or elastic waves.
  - Conductivity imaging: sensitivity to only the electrical contrast.
  - Spatial resolution: low.
  - Hybrid imaging: Conductivity imaging gives its contrast and acoustic or elastic wave its spatial resolution.
- Spectroscopic tissue property imaging: specific dependence with respect to the frequency of the contrast.
  - Detect the characteristic signature of tumors; determine which are malignant and which are benign: specificity enhancement.
  - Classify micro-structure organization using spectroscopic tissue property imaging: resolution enhancement.
- Plasmonic imaging: take advantage of scattering and absorption enhancements and single particle imaging.

Mathematics for biomedical imaging

- Anomaly imaging:
  - Conductivity anomalies.
  - Ultrasound and microwave anomalies.
  - Elastic anomalies.
- Hybrid imaging:
  - Acousto-electric effect:
  - Ultrasound-modulated optical tomography;
  - Ultrasonically-induced Lorentz force electrical impedance tomography.
- Spectroscopic imaging:
  - Bio-inspired dictionary matching based approach.
  - Spectroscopic electrical tissue property imaging.

Acousto-electric imaging

- Acousto-electric effect:
  - Acoustic pressure: $p(x,t) = p_0 b(x) a(t)$; p_0: amplitude; b: beam pattern; a: ultrasound waveform.
  - Acousto-electric effect:

$$\Delta\sigma = \eta\sigma p; \quad \eta: \text{ interaction constant.}$$

- Acousto-electric imaging:
  - Change of conductivity induces a change of the boundary voltage measurements.
  - Scan the sample, record the boundary variations, and determine the conductivity distribution.

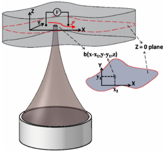

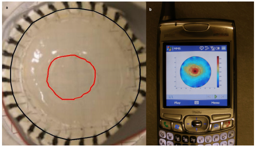

Acousto-electric imaging

- Acousto-electric imaging: mathematical and numerical framework.
- u the voltage potential induced by a current g in the absence of acoustic perturbations:

$$\begin{cases} \nabla_x \cdot (\sigma(x) \nabla_x u) = 0 \text{ in } \Omega \,, \\ \sigma(x) \dfrac{\partial u}{\partial \nu} = g \text{ on } \partial\Omega \,. \end{cases}$$

- Suppose σ bounded from below and above and known in a neighborhood of the boundary $\partial\Omega$: $\sigma = \sigma_\star$; Set $\Omega' \subset \Omega$ where σ is unknown.

Acousto-electric imaging

- Use of focalized ultrasonic waves with D as a focal spot $\rightarrow$

$$\sigma_\delta(x) \quad = \quad \sigma(x)\Big[1+\chi(D)(x)\,(\nu(x)-1)\Big],$$

  with $\nu(x)=\eta p(x)$: known.

- u_δ induced by g in the presence of acoustic perturbations localized in the focal spot $D := z+\delta B$:

$$\begin{cases} \nabla_x \cdot (\sigma_\delta(x)\nabla_x u_\delta(x)) = 0 \text{ in } \Omega, \\ \sigma(x)\dfrac{\partial u_\delta}{\partial \nu} = g \text{ on } \partial\Omega. \end{cases}$$

Acousto-electric imaging

- Suppose the focal spot D to be a disk and $u \in W^{2,\infty}(D)$. Then,

$$\int_{\partial\Omega} (u_\delta - u) g \, d\sigma = |\nabla u(z)|^2 \int_D \sigma(x) \frac{(\nu(x) - 1)^2}{\nu(x) + 1} dx$$
$$+ O(|D|^{1+\beta}),$$

  - $O(|D|^{1+\beta}) \leq C|D|^{1+\beta} ||\nabla u||_{L^\infty(D)} |\nabla^2 u||_{L^\infty(D)}$ with C: independent of D and u.
  - β: depends only on Ω', ν, $\sup_\Omega \sigma, \min_\Omega \sigma$.

Acousto-electric imaging

- Suppose $\sigma \in \mathcal{C}^{0,\alpha}(D)$, $0 \leq \alpha \leq 2\beta \leq 1$. Then

$$\begin{aligned}\mathcal{E}(z) &:= \left(\int_D \frac{(\nu(x)-1)^2}{\nu(x)+1}\,dx\right)^{-1}\int_{\partial\Omega}(u_\delta - u)g\,d\sigma \\ &= \sigma(z)\,|\nabla u(z)|^2 + O(|D|^{\alpha/2}).\end{aligned}$$

- $\mathcal{E}(z)$: electrical energy density; known function from the boundary measurements.

Acousto-electric imaging

- Substitute σ by $\mathcal{E}/\left|\nabla u\right|^2$.
- Nonlinear PDE (the 0–Laplacian)

$$\left\{ \begin{array}{l} \nabla_x \cdot \left(\dfrac{\mathcal{E}}{\left|\nabla u\right|^2} \nabla u \right) = 0 \quad \text{in } \Omega , \\ \dfrac{\mathcal{E}}{\left|\nabla u\right|^2} \dfrac{\partial u}{\partial \nu} = g \quad \text{on } \partial\Omega . \end{array} \right.$$

- g such that u has no critical point inside Ω'.
- Choose two currents g_1 and g_2 s.t. $\nabla u_1 \times \nabla u_2 \neq 0$ for all $x \in \Omega$.

Acousto-electric imaging

Reconstruct the conductivity distribution knowing the internal energies:

- Linearized versions of the nonlinear (zero-Laplacian) PDE problems.
- Optimal control approach: minimize over the conductivity the discrepancy between the computed and reconstructed internal energies.
- Optimal control approach: more efficient approach specially with incomplete internal measurements of the internal energy densities.
- Resolution of order the size of the focal spot + stability (wrt measurement noise).
- Exact inversion formulas: derivatives of the data $\Rightarrow$ used only to obtain a good initial guess.

Differential imaging

- Acoustically modulated optical tomography:

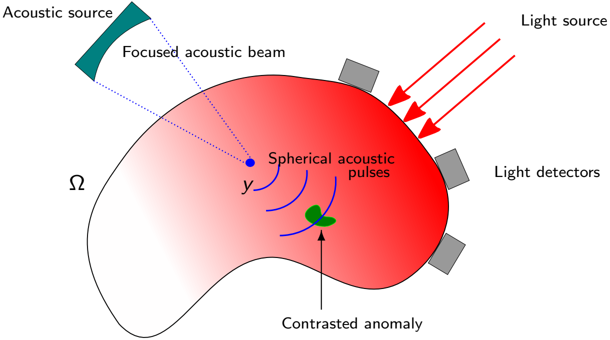

- Record the variations of the light intensity on the boundary due to the propagation of the acoustic pulses.

Differential imaging

- g: the light illumination; a: optical absorption coefficient; l: extrapolation length. Fluence Φ (in the unperturbed domain):

$$\begin{cases} -\Delta\Phi + a\Phi = 0 \quad \text{in } \Omega, \\ l\dfrac{\partial \Phi}{\partial \nu} + \Phi = g \quad \text{on } \partial\Omega. \end{cases}$$

- Acoustic pulse propagation: $a \to a_u(x) = a(x + u(x))$.
- Fluence Φ_u (in the displaced domain):

$$\begin{cases} -\Delta\Phi_u + a_u\Phi_u = 0 \quad \text{in } \Omega, \\ l\dfrac{\partial \Phi_u}{\partial \nu} + \Phi_u = g \quad \text{on } \partial\Omega. \end{cases}$$

- u: thin spherical shell growing at a constant speed; y: source point; r: radius.
- Cross-correlation formula:

$$M(y,r) := \int_{\partial\Omega} \left(\frac{\partial \Phi}{\partial \nu}\Phi_u - \frac{\partial \Phi_u}{\partial \nu}\Phi \right) = \int_\Omega (a_u - a)\Phi\Phi_u \approx \underbrace{\int_\Omega u \cdot \nabla a \, |\Phi|^2}_{\text{Taylor+Born}}.$$

Differential imaging

- Helmholtz decomposition: $\Phi^2 \nabla a = \nabla \psi + \nabla \times A$.
- Spherical Radon transform: $\nabla \psi = -\frac{1}{c} \nabla \mathcal{R}^{-1} \left[\int_0^r \frac{M(y,\rho)}{\rho^{d-2}} d\rho \right]$.
- System of nonlinearly coupled elliptic equations: $\nabla \cdot \Phi^2 \nabla a = \Delta \psi$ and $\Delta \Phi + a \Phi = 0$.
- Fixed point and Optimal control algorithms.
- Reconstruction for a realistic absorption map.
- Proofs of convergence for highly discontinuous absorption maps (bounded variation).

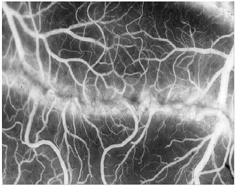

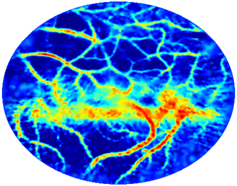

Lorentz force electrical impedance tomography

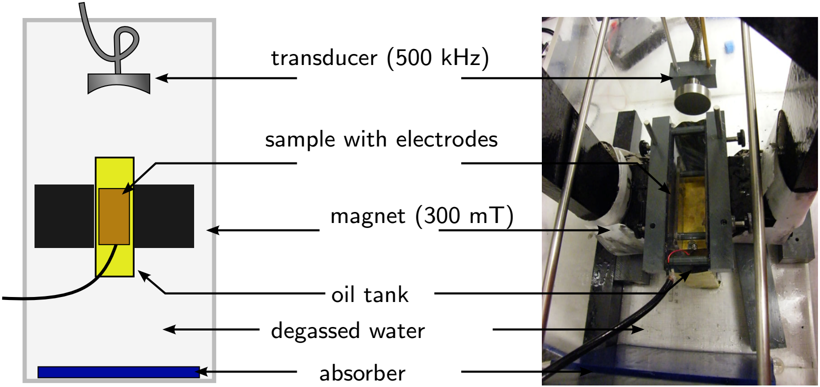

Example of the imaging device. A transducer is emitting ultrasound in a sample placed in a constant magnetic field. The induced electrical current is collected by two electrodes.

Lorentz force electrical impedance tomography

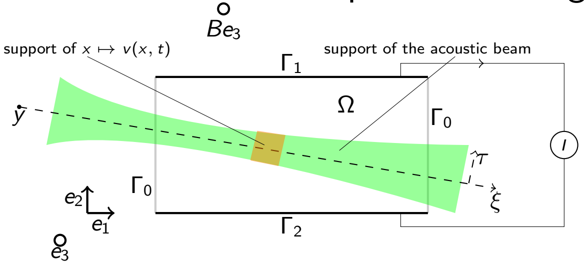

- Interaction between $v(x,t)\xi$ and Be_3: induces Lorentz' force on the ions in $\Omega \Rightarrow$ separation of charges $\equiv$ source of current and potential: $j_S(x,t) = \frac{B}{e^+}\sigma(x)v(x,t)\tau$; e^+: elementary charge.
- Voltage potential u:

$$\begin{cases} -\nabla\cdot(\sigma\nabla u) = \nabla\cdot j_S \quad \text{in } \Omega, \\ u = 0 \quad \text{on } \Gamma_1\cup\Gamma_2, \ \dfrac{\partial u}{\partial \nu} = 0 \quad \text{on } \Gamma_0. \end{cases}$$

- Measured intensity: $I(y,\xi) = \int_{\Gamma_2} \sigma \dfrac{\partial u}{\partial \nu}$.

Lorentz force electrical impedance tomography

- Virtual potential:

$$U := F[\sigma] = \begin{cases} -\nabla \cdot (\sigma \nabla U) = 0 & \text{in } \Omega, \\ U = 0 & \text{on } \Gamma_1, \\ U = 1 & \text{on } \Gamma_2, \\ \partial_\nu U = 0 & \text{on } \Gamma_0. \end{cases}$$

- Wiener deconvolution filter: recover $J(x) = (\sigma \nabla U)(x)$ from measured intensities $I(y, \xi)$.
- Recover σ from $J = \sigma \nabla U$.
- Optimal control algorithm:
  - $\min_{\sigma} \int_{\Omega} |\sigma \nabla F[\sigma] - J|^2 +$ regularization term (a prior).
  - Nonconvexity (numerically); high sensitivity to noise.

Lorentz force electrical impedance tomography

Direct method

- Viscosity-type regularization method:

$$\begin{cases} \nabla \cdot (\varepsilon I + (J^\perp (J^\perp)^T)\nabla U_\varepsilon = 0 & \text{in } \Omega, \\ U_\varepsilon = x_2 & \text{on } \partial\Omega. \end{cases}$$

- Reconstructed image:

$$\frac{1}{\sigma_\varepsilon} := \frac{J^\perp \cdot \nabla U_\varepsilon}{|J|^2} \to \frac{1}{\sigma} \text{in } L^2$$

as the viscosity parameter $\varepsilon \to 0$.

Lorentz force electrical impedance tomography

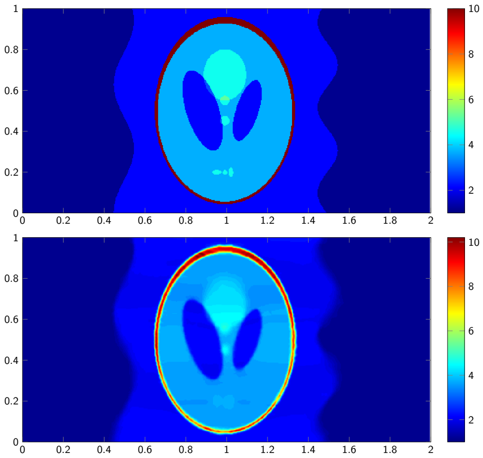

Lorentz force electrical impedance tomography

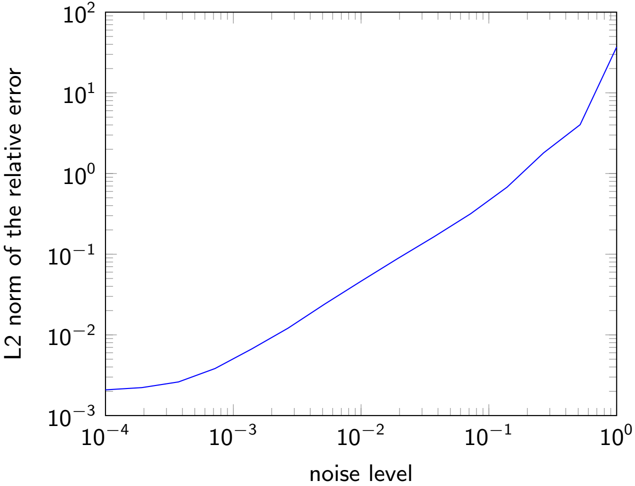

Bio-inspired dictionary matching based approach

- Electrolocation for weakly electric fish:
  - Electric organ: generate a stable, high-frequency, weak electric field.
  - Electroreceptors: measure the transdermal potential modulations caused by a nearby target.
  - Nervous system: perceive target's shape.

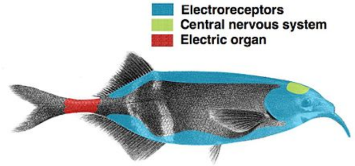

Bio-inspired dictionary matching based approach

Mechanism for imaging:

- Form an image from the perturbations of the field due to targets.
- Identify and classify the target, knowing by advance that it belongs to a learned dictionary of shapes.
  - Extract the features from the data.
  - Construct invariants with respect to rigid transformations and scaling.
  - Compare the invariants with precomputed ones for the dictionary.
- Biological targets: frequency dependent electromagnetic properties (capacitive effect generated by the cell membrane structure).
- Spectroscopic measurements of the target's polarization tensor.

Bio-inspired dictionary matching based approach

- Wave-type electric signal: $f(x,t) = f(x)\sum_n a_n e^{in\omega_0 t}$; ω_0: fundamental frequency.

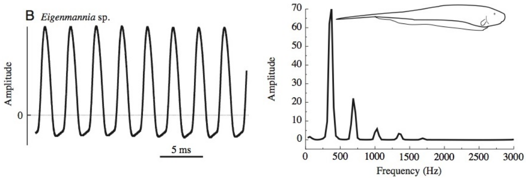

- Skin: very thin ($\delta \sim 100\mu$m) and highly resistive ($\sigma_s/\sigma_0 \sim 10^{-2}$); $\sigma_b/\sigma_0 \sim 10^2$ (highly conductive).

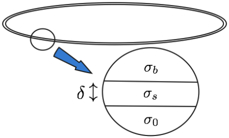

Bio-inspired dictionary matching based approach

- Target $D = z + \delta' B$; z: location; δ': characteristic size of the target; $k(\omega) = (\sigma(\omega) + i\omega\varepsilon(\omega))/\sigma_0$; k, σ, and ε: the admittivity, the conductivity, and the permittivity of the target; $\omega_n = n\omega_0$: the probing frequency.
- u_n : the electric potential field generated by the fish:

$$\begin{cases} \Delta u_n = f, & x \in \Omega, \\ \nabla \cdot (1 + (k-1)\chi(D))\nabla u_n = 0, & x \in \mathbb{R}^2 \setminus \overline{\Omega}, \\ \dfrac{\partial u_n}{\partial \nu}\Big|_- = 0, \quad [u_n] = \xi \dfrac{\partial u_n}{\partial \nu}\Big|_+ & x \in \partial\Omega, \\ |u_n(x)| = O(|x|^{-1}), & |x| \to \infty. \end{cases}$$

- $\xi := \delta\sigma_0/\sigma_s$ effective thickness.
- $\lambda(\omega) = (k(\omega) + 1)/(2(k(\omega) - 1))$.

Bio-inspired dictionary matching based approach

- Dipole approximation: $u_n(x) - U(x) \simeq \mathbf{p} \cdot \nabla G(x - z)$.
  - G: Green's function associated to Robin boundary conditions.
  - Dipole moment $\mathbf{p} = - \underbrace{M(\lambda(\omega), D)}_{\text{Polarization tensor}} \nabla U(z)$.
  - $M(\lambda(\omega), D) = \int_{\partial D} x(\lambda I - \mathcal{K}_D^*)^{-1}[\nu](x)\, ds(x)$.

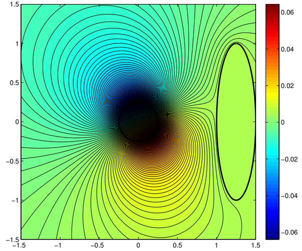

Bio-inspired dictionary matching based approach

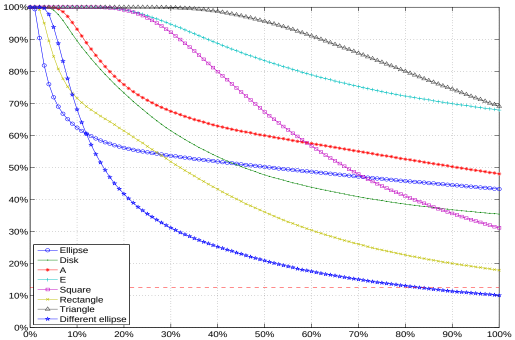

Probability of detection in terms of the noise level. Stability of classification based on differences between ratios of eigenvalues of $\Im m \, M(\lambda(\omega), D)$.

Spectroscopic electrical tissue property imaging

- Differentiate between normal, pre-cancerous and cancerous tissues from electrical measurements at tissue level.
- Frequency dependence of the (anisotropic) homogenized admittivity: $\omega \mapsto K^*(\omega)$.
- Relaxation times:
    - $1/\arg\max_\omega$ eigenvalues of $\Im m\, K^*(\omega)$;
    - Classification: invariance properties;
    - Measure of anisotropy: ratios of the eigenvalues of $\Im m\, K^*(\omega)$.

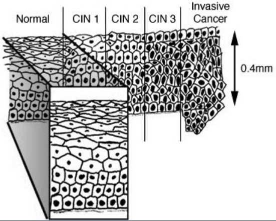

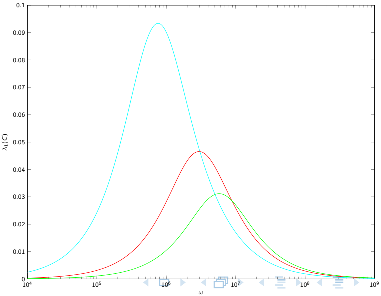

Spectroscopic electrical tissue property imaging

The effective admittivity of a periodic dilute suspension:

$$K^* = k_0 \left(I + f M \left(I - \frac{f}{2} M \right)^{-1} \right) + o(f^2).$$

- f: volume fraction; ξ: effective thickness of the membrane; ∂D: cell membrane; $\widetilde{D} = D/\sqrt{f}$: rescaled cell.
- M: membrane polarization tensor

$$M = -\left(\xi \int_{\partial \widetilde{D}} \nu_j \left(I + \xi L_{\widetilde{D}} \right)^{-1} [\nu_i](y) ds(y) \right)_{i,j=1,2}.$$

- $L_{\widetilde{D}}[\varphi](x) = \frac{1}{2\pi} \mathrm{p.v.} \int_{\partial \widetilde{D}} \frac{\partial^2 \ln |x-y|}{\partial \nu(x) \partial \nu(y)} \varphi(y) ds(y), \quad x \in \partial \widetilde{D}.$

Spectroscopic electrical tissue property imaging

- Properties of the membrane polarization tensor:
  - M: symmetric; invariant by translation;
  - $M(sC, \xi) = s^2 M(C, \frac{\xi}{s})$ for any scaling parameter $s > 0$.
  - $M(\mathcal{R}C, \xi) = \mathcal{R}M(C, \xi)\mathcal{R}^t$ for any rotation $\mathcal{R}$.
  - $\Im m\, M$ is positive and its eigenvalues, $\lambda_1 \geq \lambda_2$, have one maximum with respect to ω.
- Relaxation times for the arbitrary-shaped cells:

$$\frac{1}{\tau_i} := \arg\max_{\omega} \lambda_i(\omega).$$

- $(\tau_i)_{i=1,2}$: invariant by translation, rotation and scaling.
- Concentric circular-shaped cells: Maxwell-Wagner-Fricke formula ($\lambda_1 = \lambda_2$).
- Nondilute regime: Assume f known $\Rightarrow$ Classification based on relaxation times.

Plasmonic resonant nanoparticles

- Gold nano-particles: accumulate selectively in tumor cells; bio-compatible; reduced toxicity.
- Detection: localized enhancement in radiation dose (strong scattering).
- Ablation: localized damage (strong absorption).
- Functionalization: targeted drugs.

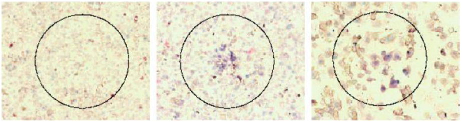

M.A. El-Sayed et al.

Plasmonic nanoparticles

- D: nanoparticle; ν: normal to ∂D; $\varepsilon(\omega)$: complex permittivity contrast; $\lambda(\omega) = (\varepsilon(\omega)+1)/(2(\varepsilon(\omega)-1))$.
- Neumann-Poincaré operator $\mathcal{K}_D^*$:

$$\mathcal{K}_D^*[\varphi](x) = \frac{1}{2\pi} \int_{\partial D} \frac{\langle x-y, \nu_x \rangle}{|x-y|^2} \varphi(y)\, ds(y) \,, \quad x \in \partial D.$$

- Symmetrization technique (Calderón's identity): Discrete spectrum $\sigma(\mathcal{K}_D^*)$ in $]-1/2, 1/2[$.
- Quasi-static plasmonic resonance: $\mathrm{dist}(\lambda(\omega), \sigma(\mathcal{K}_D^*))$ minimal ($\Re e\, \varepsilon(\omega) < 0$).
- Enhancement of the absorption and scattering cross-sections Q^a and Q^s at plasmonic resonances:

$$Q^a + Q^s \propto \Im m\, \mathrm{Trace}(M(\lambda(\omega), D)); \; Q^s \propto \left| \mathrm{Trace}(M(\lambda(\omega), D)) \right|^2.$$

- Polarization tensor: $M(\lambda(\omega), D) := \int_{\partial D} x (\lambda(\omega) I - \mathcal{K}_D^*)^{-1}[\nu](x)\, ds(x).$

Plasmonic nanoparticles

- $\mathcal{K}_D^*$: scale invariant $\Rightarrow$ Quasi-static plasmonic resonances: size independent.
- Analytic formula for the first-order correction to quasi-static plasmonic resonances in terms of the particle's characteristic size δ:

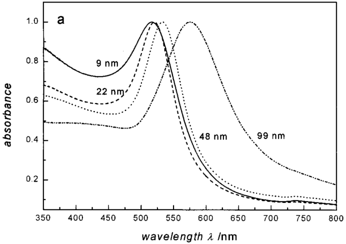

M.A. El-Sayed et al.

- Operator-Valued function $\delta \mapsto \mathcal{A}_\delta(\omega)$:

$$\mathcal{A}_\delta(\omega) = \overbrace{(\lambda(\omega)I - \mathcal{K}_D^*)}^{\mathcal{A}_0(\omega)} + (\omega\delta)^2 \mathcal{A}_1(\omega) + O((\omega\delta)^3).$$

Resonant media for super-resolution

- Super-resolution for plasmonic nanoparticles:

S. Nicosia & C. Ciraci, Cover, Science 2012

Plasmonic nanoparticles

- Resolution: determined by the behavior of the imaginary part of the Green function. Helmholtz-Kirchhoff identity:

$$\Im m\, G(x, x_0, \omega) = \omega \int_{|y|=R} \overline{G(y, x_0, \omega)} G(x, y, \omega) ds(y), \quad R \to +\infty.$$

- The sharper is $\Im m\, G$, the better is the resolution.
- Local resonant media used to make shape peaks of $\Im m\, G$.
- Mechanism of super-resolution in resonant media:
  - Interaction of the point source x_0 with the plasmonic nanoparticles excites high-modes.
  - Resonant modes encode the information about the point source and can propagate into the far-field.
  - Super-resolution: only limited by the resonant structure and the signal-to-noise ratio in the data.

Plan

Resolution, stability, and specificity enhancement:

- Anomaly imaging: scale separation techniques; model reduction;
- Hybrid (or multi-wave) imaging: different types of waves are combined into one imaging system;
- Spectroscopic imaging: source separation techniques;
- Physic-based learning approach: data representation; feature extraction;
- Nanoparticle imaging: scattering and absorption enhancement; single particle imaging.

Mathematical and probabilistic tools:

- Singular-value decomposition; regularization; random media; integral transforms; Kramers-Kronig relations; optimal control;
- Layer potential techniques; asymptotic analysis; spectral analysis.